Encapsulation of alkyl and aryl derivatives of quaternary ammonium cations within Cucurbit[n]uril (n=6,7) and their inverted diastereomers: Density Functional Investigations

---

Ishita A. Raja[a], Vivekanand V. Gobre[b], Rahul V. Pinjari[c], Shridhar P. Gejji[a,*]

[a]*Department of Chemistry, University of Pune, Ganeshkhind, Pune 411007 India.*

[b]*Fritz Haber Institute of the Max Planck Society,Faradayweg 4-6, D-14195 Berlin-Dahlem,Germany.*

[c]*School of Chemical Sciences, Swami Ramanand Teerth Marathwada University, Nanded 431606 India.*

*Corresponding Author: spgejji@chem.unipune.ac.in

Fax No. : +91–020–225691728

Abstract

Electronic structure, vibrational frequencies and ^{1}H chemical shifts of inclusion complexes between CB[n] (n=6,7) or their inverted *i*CB[n] diastereomer hosts and quaternary diammonium viz., 1,6-hexyldiammonium (HDA) or p-xylyldiammonium (XYL) cationic guests are obtained from the density functional calculations. The interaction of CB[n] or *i*CB[n] with HDA (guest) conduce inclusion complexes in which the guest attains gauche conformation within the host cavity. The lowest energy XYL complexes of CB[6] or *i*CB[6] are comprised of one ammonium group orienting parallel to aromatic ring. The CB[7] or *i*CB[7] complexes of XYL on the other hand, reveal ammonium group(s) perpendicular to aromatic ring of the guest. The ureido C=O and N-H stretching vibrations on complexation engender frequency down-shift in the calculated spectra. This can be attributed to C-H---O and N-H---O interactions in the complex. The inverting of glycouril unit in *i*CB[n] renders a frequency shift (12 cm^{-1}) for the C=O stretching in the opposite direction. Molecular electron density topography and natural bond orbital analyses have been used to explain the direction of frequency shifts. Calculated ^{1}H NMR reveal that guest protons within the host cavity not participating in hydrogen bonding interactions, exhibit shielded signals compared to isolated XYL or HDA. Likewise the inverted protons in the *i*CB[6]-XYL complex led to up-field signals in calculated ^{1}H NMR as a result of C-H---π interactions.

Keywords: Inclusion complex, inverted cucurbit[n]urils, NMR chemical shifts, Electron density topography, Vibration Frequency.

Introduction

A family of cucurbit[n]uril, CB[n], hosts comprising of methylene-bridged glycouril units have attracted considerable attention owing to their potential applications in organic synthesis[1-4], molecular recognition[5,6], nanoscience [7,8], catalysis [9-11], drug delivery vehicles [12] and separation technology [13,14]. The number of glycouril units in cucucrbituril homologues renders varying size to their hydrophobic cavity while portal carbonyl groups on portals provide hydrophilic exterior to these macrocycles. The CB[n] macrocycles show efficient and selective binding toward simple gaseous molecules [3], aliphatic/aromatic cations [16-21], metal complexes [22-26] and macromolecules [27-30] conducing inclusion complexes. These guest molecules encapsulate within CB[n] *via* noncovalent interactions. Synthesis of CB[n] hosts has been carried out by acid catalyzed condensation reaction of glycouril and formaldehyde. The CB[n] hosts are isolated and X-ray crystallography experiments [31] elucidated their crystal structures. These authors employed ^{1}H NMR and mass spectroscopy experiments to characterize CB[n] homologues [31]. Subsequently Day *et al.* [32] investigated the underlying mechanism accompanying the formation of CB[n]. To this end, the electron spray mass spectroscopy and ^{13}C NMR experiments [32] are used to identify individual cucurbiturils in reaction mixtures. Remarkable enough, it has been shown that [33], CB[n] (n=5-8, 10) macrocycles are endowed with exceptional macrocycle acceptor ability in aqueous solution. Excellent reviews on synthesis, characterization, molecular recognition properties of cucurbituril and the exceptional strength of their interaction with a variety of guests can be found in the recent literature [34-36].

Semiempirical quantum chemical investigations on novel tubular nanostructures of modified CB[n] combined with transition metals have been reported [37]. Furthermore density functional theory have been successfully applied to characterize the electronic structure and spectral

features of CB[n] homologues and modified CB[n] hosts [37-44]. It has been inferred that CB[6] or CB[7] allows binding of various guests of appropriate length and size [45-47].

It should be remarked here that during the synthesis of cucurbit[n]urils Isaacs and coworkers isolated [48-50] intermediates, in which one (or two) of the glycouril units of CB[n] is(/are) inverted with its the methine protons residing within the host cavity. These kinetic products are referred as inverted cucurbit[n]urils (*i*CB[n]). A prototype *i*CB[7] host is shown schematically in Fig. 1. Gejji and Pinjari [44] derived electronic structure, molecular electrostatic potentials and NMR chemical shifts in i^x-CB[n] (n=6,7, x=1,2), diastereomers of CB[n]. These authors demonstrated that i^x-CB[n] hosts reveal distinct features in their charge distribution [44] and thus should exhibit qualitatively different host guest binding patterns than their parent CB[n] analogues. It has also been pointed out that inverting of one (or two) glycouril unit(s) of CB[n] hosts (n=6-8) engender enhanced dipole moment [50]. The i^x-CB[n] diastereomers (x=1 or 2; n=6-8) are found to be stable in gas phase and in different solvents. ^{1}H NMR patterns of isolated *i*CB[6] and *i*CB[7] from the density functional calculations agree well with experimentally measured NMR spectra [44]. Nonetheless, reports on complexation of i^x-CB[n] hosts are scanty. Only a few systems describing encapsulation of aliphatic as well as aromatic cation are reported to date [50].

Developing synthetic receptor for selective molecular recognition of ammonium cation is crucial in chemistry and molecular biology [51]. It is known that the size-complementarities of the host cavity and the guest govern the host-guest binding. The dimensions of CB[6] cavity are comparable to those of *para*-substituted benzene ring, hence the CB[6] or modified CB[6] macrocycle efficiently encapsulates biologically important amines, *para*-xylyldiammonium (XYL) cation and quaternary ammonium ions. The interaction of these hosts and quaternary

ammonium cations stem from hydrogen bonding. In addition, electrostatic and cation-π interactions [51] contribute toward such binding. The present work analyzes how complexation of CB[n] or *i*CB[n] with 1,6-hexyldiammonium (HDA) or xylyldiammonium (XYL) cationic guests, prototype representatives of aliphatic and aromatic molecular systems, respectively, influences ^{1}H NMR of the isolated host or the guest. Since the reorganization of electron density subsequent to complexation brings about alteration in bond-strength of individual guest and the host, the frequency shifts in their vibrational spectra have been studied by the density functional theory.

Computational Method

Geometry optimizations of inclusion complexes of CB[n] and *i*CB[n] hosts with aliphatic HDA and aromatic XYL di-cation guests were carried out within the realm of density functional theory using Becke97-D (B97D) functional due to Grimme and coworkers [52,53] employing the GAUSSIAN09 program [54]. The internally stored 6-31+G(d,p) basis set were used. We further carried out calculations by extending the basis set with addition of diffuse functions on hydrogen atoms in these molecular systems. Use of the B97D exchange correlation functional accounts for the dispersive interactions underlying the host-guest binding. Furthermore the density functional optimizations based on M06-2X exchange-correlation functional [55] were carried out for the CB[n]-HDA and *i*CB[n]-XYL (n=6) complexes. The molecular electrostatic potential (MESP) topography in the isolated CB[n] hosts and their inverted analogs were computed using the locally written program in our laboratory. The vibrational frequencies of the lowest energy complexes were obtained from the computations incorporating the 6-31G(d,p) basis set. The lowest energy structures of complexes thus obtained were characterized as local minima by examining the number of imaginary frequencies. All normal vibrations frequencies for these

structures turn out to be real which confirm them as local minima. These normal vibrations were assigned by visualizing displacements of atoms around their equilibrium (mean) positions employing the program GAUSSVIEW [56]. Molecular electron density (MED) topography was computed using the Quantum Theory of Atoms in Molecule (QTAIM) proposed by Bader [57,58]. The bond critical points (bcp) were thus identified using the locally written UNIVIS-2000 [59] program. The hydrogen bonding interactions underlying the conducing of inclusion complex emerge with the (3,-1) bond critical points (bcp) as their signature. Thus the calculated $\Delta\rho$ are utilized to gauge variation in the bond strength. NMR chemical shifts (δ) are calculated by subtracting the nuclear magnetic shielding tensors of protons in molecules of interest from those in teramethyl silane, TMS, (as a reference) using the gauge invariant atomic orbital method [60]. Effect of solvent (water) on relative energies of CB[n] or *i*CB[n] and their complexes was simulated by using the self-consistent reaction field theory incorporating the polarizable continuum model (SCRF-PCM) [61]. The influence of solvent on chemical shifts (δ_H) in the ^{1}H NMR spectra has further been analyzed [38, 44].

Results and discussion

To understand interactions of HDA and XYL with CB[n] or *i*CB[n] (n =6, 7) we consider different conformers of host-guest inclusion complexes. The conformation search was guided by the molecular electrostatic potential topography of isolated CB[n] and *i*CB[n] hosts. The (3,+3) critical points representing the minima in the MESP topography serve as binding site for the guest. With this view, HDA and XYL different conformers of CB[n] or *i*CB[n] complexes were generated with the rotation and translation of the guest in the neighborhood of the MESP minima within the isolated host. Only the conformers exhibiting qualitatively different host-guest binding patterns, shown in Fig. 1S and Fig. 2S of supporting information, were subjected to

optimizations using the B97D based density functional calculations. Some of these conformers converged to nearly identical stationary point geometries. In following discussion conformers with increasing relative stabilization energies, are denoted by CB[n]-guest-X, and *i*CB[n]-guest-X (guest= XYL/HDA, n = 6, 7 and X =A, B, C). The lowest energy complex of CB[n] or *i*CB[n] with guest (HDA or XYL), thus is denoted by CB[n]-guest-A or *i*CB[n]-guest-A. Atom numbering scheme in the monomer has been displayed in Fig. 2.

It has been noticed that the lowest energy inclusion complexes of CB[n] or *i*CB[n] host reveals HDA in gauche conformation while XYL complexes of CB[6] and *i*CB[6] show (Fig. 2S of supporting information) one or both ammonium group(s) parallel to aromatic ring of guest. This partly has been attributed to relatively small cavity dimensions of these hosts. On the other hand, CB[7] and *i*CB[7] complexes possess ammonium group(s) of XYL residing perpendicular to aromatic ring of the guest. Subsequent SCRF-PCM calculations showed that the stability of the inclusion complex has not been influenced by the presence of solvent (water) and the binding patterns of host guest interactions remains unaltered.

Relative stabilization energies (ΔE_{Rel}) and binding energies (ΔE_{Bind}) of the inclusion complexes in gas phase and in water are given in Table 2. Binding energies (ΔE_{Bind}) with different basis sets are compared in Table 1. Thus, it may be inferred that the XYL binds strongly to CB[n] or *i*CB[n] hosts than HDA. As shown in Table 2, ΔE_{Bind} for the HDA and XYL complexes are lowered considerably in aqueous solution. The binding energy of CB[6]-HDA-A complex decreases from 651.7 kJ mol^{-1} to 220.9 kJ mol^{-1} in the presence of water. It should further be remarked here that the M06-2X based density functional calculations are gaining popularity in these years [55]. The hitherto exchange correlation functional well describes the dispersive interactions in noncovalent host-guest binding. As pointed out earlier in the preceding section on

the computational method we carried out the M06-2X/6-31++G(d,p) calculations on the CB[6]-HDA-A and *i*CB[6]-XYL-A conformers as test cases. The selected hydrogen bond distance parameters of these conformers derived from the M06 and B97D calculations are compared in Table 6S of supplementary information. Thus, excellent qualitative agreement from these two calculations is transparent from superimposed structures obtained from these two methods shown in figure 5S of supplementary information. The M06-2X functional leads to slower convergence for optimization of the inclusion complex. The respective binding energies of the CB[6]-HDA and *i*CB[6]-XYL complexes from the M06-2X theory are predicted to be 673 and 651 kJ mol^{-1} which compares well with those from the B97D calculations (*cf.* Table 1). Besides this, calculated binding energies reported in Table 1, clearly points out that binding energies are nearly insensitive to change of basis from the 6-31+G(d,p) to 6-31++G(d,p) basis.

Electron densities at the bond critical point (Fig.3) (ρ_{bcp}) in the MED topography in XYL and HDA complexes of CB[n] and *i*CB[n] are given in Table 3. Here, ρ_{bcp} emerges as a signature of the hydrogen bonding interactions underlying host-guest binding. The ρ_{bcp} values of hydrogen bonds in XYL and HDA inclusion complexes of CB[n] and *i*CB[n] are compared in Table 3.The strength of hydrogen-bonding interactions can be gauged from these ρ_{bcp} values. Thus, *six* N-H---O interactions are inferred in the minimum energy inclusion complexes of HDA as well as XYL. It is thus evident that N-H---O interactions in CB[7] or *i*CB[7] inclusion complexes prevail over those in their lower homologues. In addition to this, CB[6] and *i*CB[6] facilitate stronger C-H---O interactions in their complexes owing to small cavity-dimensions of the host. Except for the *i*CB[7]-XYL complex by and large, the CB[7] and *i*CB[7] complexes are void of C-H---O interactions. (*cf.* Table 3)

As pointed out in the preceding section, the vibrational frequencies of CB[n]-HDA(/XYL)-A and *i*CB[n]-HDA(/XYL)-A minimum energy complexes have been obtained within the framework of B97D/6-31G(d,p) theory. Selected vibrational frequencies of XYL, CB[n] and *i*CB[n] hosts and their minimum energy complexes are reported in Table 5. The vibrational spectra in different regions, viz., (a) 3500 cm^{-1} - 2700 cm^{-1} (b) 2000 cm^{-1} - 1500 cm^{-1} (c) 1500 cm^{-1} - 1000 cm^{-1} (d) 1000 cm^{-1} - 500 cm^{-1} and (e) below 500 cm^{-1} are depicted in Fig. 4S of supporting information. Further the complexes (depicted in **red)** in (a)-(e) wave number regions are compared with those of isolated host (black) and guest (blue) in this figure.

XYL encapsulated CB [6] or iCB[6]

As shown in fig 4S(1) a near doublet (3354 cm^{-1} and 3339 cm^{-1}) of comparable intensities, assigned to NH stretching is observed for the isolated XYL. On complexation with CB[6] the higher wave number vibration of these reveals a blue-shift of ~27 cm^{-1}. As opposed to this, the ~3205 cm^{-1} band of aromatic guest shows a frequency shift in the opposite direction, attributed to N-H---O interactions and accordingly this vibration appears at the ~3150 cm^{-1} in the lowest energy CB[6]-XYL complex. On inverting one glycouril unit (as in *i*CB[6]) the corresponding the NH stretching vibration appears at the 3339 cm^{-1} which moves to 3369 cm^{-1} on complexation with XYL (*cf.* Figure 4S(2)) Owing to N-H---O interactions NH stretching at 3205 cm^{-1} of the isolated XYL exhibit a shift to lower wave number (3149 cm^{-1}) in the *i*CB[6] complex.

As depicted in fig 4S(1)(b) the carbonyl (C=O) stretching of the isolated CB[6] assigned to 1782 cm^{-1} vibration reveals red-shift and this vibration shifts to 1748 cm^{-1} in the CB[6]-XYL-A complex. Likewise, the complexation of *i*CB[6] predicts a shift from 1779 cm^{-1} to 1755 cm^{-1} for the corresponding vibration. Thus, relatively stronger C=O---H interactions can be inferred

for the CB[6] complex. Remarkably enough, the C=O stretching vibration from the inverted glycouril unit of *i*CB[6] do not exhibit frequency down shift since this functionality do not facilitate hydrogen bonding interactions in its complex.

XYL encapsulated CB[7] or iCB[7]

The N-H stretching vibrations in 3500 cm^{-1} -2700 cm^{-1} region which facilitating hydrogen bonding host-guest interactions reveal a down-shift to 3120 cm^{-1} whereas those which do not participate in such interactions engender a band at the ~3360 cm^{-1} in the lowest energy CB[7]-XYL complex as shown in Figure 4S(3)(a). Similar inferences are drawn for the *i*CB[7]-XYL-A analog. Interestingly NH stretching vibration comprising of protons not participating in hydrogen bonding moves from 3354 cm^{-1} to 3366 cm^{-1} (*cf.* fig 4S(4)(a)). Consequent to N-H---O interactions a down shift from 3205 cm^{-1} to 3150 cm^{-1} for the N-H stretching in the *i*CB[7]-XYL complex was observed. Furthermore, the methylene stretching vibration in the CB[7] assigned to an intense band near the 2860 cm^{-1} corresponds to 2911 cm^{-1} band in the XYL encapsulated CB[7] complex. Likewise the *i*CB[7] and its XYL complex reveal the corresponding vibrations at the 2862 cm^{-1} and 2923 cm^{-1}, respectively, as depicted in figure 4S-4(a). As may readily be noticed, the 1700 cm^{-1} -1800 cm^{-1} region reveals complexation with XYL leads to a downshift of 9 cm^{-1} for the intense carbonyl stretching (1777 cm^{-1}) in CB[7] (*cf.* fig 4S(3)). A comparison with the inverted CB[7] complex, predicts relatively large frequency red-shift for the 1776 cm^{-1} (C=O stretching) band of isolated *i*CB[7] (*cf.* fig 4s(4)). Thus, stronger hydrogen bonding interactions are inferred for the *i*CB[7] complex relative to its un-inverted counterpart contrary to the case of CB[6] or *i*CB[6] complexes discussed earlier.

Calculated vibrational spectra of isolated HDA and its complexes with CB[n] and *i*CB[n] are displayed in Fig. 3S of supporting information. Selected vibrational frequencies are reported in

Table 4. The following inferences may be drawn. On encapsulation of HDA within CB[6] or CB[7] macrocycle carbonyl stretching arising from ureido groups on host portals, those facilitate C=O---H interactions engender frequency down-shift of 16 cm^{-1}. Moreover, the NH stretching vibrations participating in N-H---O interactions reveal a red-shift while those which do not participate in the N-H---O interactions engender a frequency-shift in the opposite direction thereby resulting in a blue shift in the HDA complex. The complexation of CB[n] or *i*CB[n] with HDA led to similar conclusions for the frequency-shift in the calculated spectra as inferred earlier for the XYL complexes.

CB[7] or *i*CB[7] inclusion complexes possess relatively strong N-H---O interactions as pointed out earlier. Large frequency downshift of the corresponding N-H stretching in CB[7] or *i*CB[7] complexes than its CB[6] counterpart thus has been rationalized. Moreover, ρ_{bcp} data in Table 3 suggested that CB[6] and *i*CB[6] facilitate C-H---O interactions. A large frequency red-shift of the corresponding C=O stretching in CB[6] or *i*CB[6] homologue is further evident.

To understand the direction of frequency shift of characteristics vibrations on complexation of CB[n] or *i*CB[n] hosts we carried out the natural bond orbital analyses. The electron density in anti-bonding orbital of NH and C=O bonds in isolated hosts and their complexes are summarized in Table 6. An increase of electron density in anti-bonding orbital (σ^* in au) of complexes engenders bond elongation (r in Å) leading to a downshift (red-shift) in frequency of the corresponding stretching vibration compared with isolated hosts. A frequency blue-shift of NH stretching for the NH group not participating in hydrogen bonding interactions further can be explained from the decreased electron density in its anti-bonding orbital. Thus the shortening of the corresponding bond can be noticed.

The influence of quaternary ammonium guest (XYL/HDA) encapsulation within host cavity on ^{1}H NMR chemical shifts has been outlined below. The CB[n] hosts possess three chemically nonequivalent sets of protons viz., methylene protons (H1 and H2) and methine protons denoted by H3 (Fig. 1 and Fig. 2). As pointed out in the literature, ^{1}H NMR chemical shifts (δ_H) of CB[n] and *i*CB[n] host protons calculated in gas phase and in the present of water as solvent within SCRF-PCM framework of theory which agree better, than those derived for the gas phase [44]. The δ_H values (maximum and minimum for the given type of protons) of host protons in XYL or HDA encapsulated CB[n] and *i*CB[n] complexes in water shown by parentheses in Table 7 and those of guest protons in complexes are given in Table 8.

Calculated chemical shifts of individual host protons in complexes are displayed in Table 2S to Table 5S of the supporting information. Accordingly H1, H2 and H3 protons of the CB[n], n = 6/7, in gas phase are predicted near 6.4, 3.5 and 4.8 ppm, respectively (Table 7). Encapsulation of HDA in CB[6] cavity engenders shielding of H1 protons. The H2 proton on the other hand, exhibit deshielding and show up the δ_H signals near 3.8 ppm. Similar conclusions may be drawn for HDA complexed with CB[7], *i*CB[6], and *i*CB[7] hosts. The inversion of the glycouril unit engenders splitting of these signals. Likewise, the inverted protons (for *i*CB[6] and *i*CB[7]) can be easily distinguished. The inverted protons of host further reveal an upshift in δ_H signals in *i*CB[6]-HDA-A and in *i*CB[7]-HDA-A after complexation.

A comparison of ^{1}H NMR chemical shifts in *i*CB[n] hosts with those of their inclusion complexes has been briefly discussed in the following. A significant shielding of the inverted protons was noticed in *i*CB[n]-XYL-A complexes compared to 3.5 and 4.3 ppm respectively in the calculated spectra of *i*CB[6] and *i*CB[7] hosts. Further a large up-shift of inverted H3 protons stems from C-H---π interactions with XYL aromatic ring. How complexation influences δ_H

patterns of the host as well as the guest, those of H1 (red), H2 (blue) and H3 (black) protons, is transparent from Fig. 4. Calculated spectra of CB[n] or *i*CB[n] hosts complexed with XYL, reveal qualitatively similar trend as that for host protons in the *i*CB[n]-HDA complexes.

Effect of HDA/XYL encapsulation within the host cavity on ^{1}H NMR chemical shifts of guest can be analyzed from the data given in Table 8. XYL possess three different sets of protons, *viz.* amine protons, methylene protons and aromatic protons. Out of which amine protons participate in the host-guest interactions *via* N-H---O hydrogen bonding. The **bold** values refer to protons which interact with ureido oxygens in CB[n]/*i*CB[n] portals, exhibit deshielding on complexation unlike rest of the N-H protons. For XYL complex, all methylene protons facilitate C-H---O interactions with ureido oxygen of CB[6] (owing to relatively small cavity size of host) and thus significant deshielding has been observed in its calculated spectra. The protons confined within the host cavity are shielded. Thus, δ_H values of aromatic protons are predicted near 8.0 ppm for the isolated guest; while those in CB[6]-XYL complex appear in the 6.5 to 7.1 ppm range. The complexation of XYL with the CB[7] leads to comparatively less (7.0 ppm - 7.3 ppm) shielding. Similar inferences are drawn for the *i*CB[n] complexes. As may further be noticed, on complexation HDA protons those facilitate N-H---O interactions exhibit deshielded signals in the calculated ^{1}H NMR. The methylene protons in proximity of the host on the other hand, engender large shielding. The orientation of the guest within the host cavity reflects in ^{1}H NMR spectra.

Conclusions

Systematic investigations on CB[n] or *i*CB[n] (n=6,7) complexes of aliphatic (HDA) and aromatic (XYL) cations have been carried out within the B97D/6-31+G(d,p) and B97D/6-31G(d,p) frameworks of theory. The following conclusions are drawn.

(i) HDA attains gauche conformation on its encapsulation in CB[n] or *i*CB[n] macrocycle. The stability of these complexes is governed by number of hydrogen bonding interactions. (ii) The smaller size of CB[6] or *i*CB[6] cavity accommodates XYL with ammonium groups parallel to aromatic ring of the guest while CB[7] or *i*CB[7] complexes reveal ammonium group to be perpendicular to aromatic ring as in the isolated XYL. The complexes in the gas phase and in the presence of water exhibit similar host-guest binding patterns. (iii) QTAIM theory was utilized to analyze hydrogen bonding interactions. The electron densities at the bond critical point corresponding to the hydrogen bonds shown to correlate well with hydrogen bond distances. (iv) Calculated vibration frequencies reveal that C=O stretching from the host facilitate C=O---H interactions and thus engender frequency shift to the lower wave number (red shift), unlike the carbonyl groups (C=O) of inverted glycourils, which is accompanied by a frequency shift in the opposite direction (blue shift). Moreover, C-H and N-H stretching vibrations of the quaternary diammonium guest result in frequency red-shift on complexation with the macrocycle. This can be attributed to N-H---O and C-H---O interactions. (v) ^{1}H NMR have shown that amine protons of the guest, those participate in hydrogen bonding interactions with uriedo oxygens are deshielded. On the other hand, shielding of inverted protons emerge as signature of the host-guest interactions and thus can be distinguished from those of uninverted glycouril units. Interestingly, the protons from C-H---π interactions of aromatic guest (XYL) on complexation show relatively large shielding in the ^{1}H NMR. The δ_H values of protons facilitating hydrogen bonding are less influenced by solvation.

Supporting Information

Figures of Optimized Geometries, superimposed structures of CB[6]-HDA as well as *i*CB[6]-XYL from the B97D and M06-2X functionals based DFT optimizations, vibration spectra and Tables showing ^{1}H NMR chemical shifts for host protons.

Acknowledgements

S. P. G. acknowledges support from the University Grants Commission (UGC), New Delhi, India [Research Project F34–370] and University of Pune. I. A. R. is grateful to Center for Nanomaterials and Quantum Systems (CNQS), University of Pune, for the award of research fellowship.

References

1. Jon SY, Ko YH, Park SH, Kim HJ, Kim K (2001) A facile, stereoselective [2+2] photoreaction mediated by cucurbit[8]uril. Chem. Commun 1938-1939.
2. Wang R, Yuan L, Macartney DH (2006) Cucurbit[7]uril Mediates the Stereoselective [4+4] Photodimerization of 2-Aminopyridine Hydrochloride in Aqueous Solution. J. Org. Chem 71:237-1239.
3. Wu XL, Luo L, Lei L, Liao GH, Wu LZ, Tung CH (2008) Highly Efficient Cucurbit[8]uril-Templated Intramolecular Photocycloaddition of 2-Naphthalene-Labeled Poly(ethylene glycol) in Aqueous Solution. J. Org. Chem 73:491-494.
4. Pattabiraman M, Kaanumalle LS, Natarajan A, Ramamurthy V (2006) Regioselective Photodimerization of Cinnamic Acids in Water: Templation with Cucurbiturils. Langmuir 22:7605-7609.
5. Mukhopadhyay P, Wu A, Isaacs L (2004) Social Self-Sorting in Aqueous Solution. J. Org. Chem 69:6157-6164.
6. Burnett CA, Witt D, Fettinger JC, Isaacs L (2003) Acyclic Congener of Cucurbituril: Synthesis and Recognition Properties. J. Org. Chem 68:6184-6191.
7. Balzani V, Credi A, Raymo FM, Stoddart JF (2000) Artificial Molecular Machines. Angew. Chem. Int. Ed 39:3348-3391.
8. Corma A, García H, Montes-Navajas P, Primo A, Calvino JJ, Trasobares S (2007) Gold Nanoparticles in Organic Capsules: A Supramolecular Assembly of Gold Nanoparticles and Cucurbituril. Chem. Eur. J 13:6359-6364.
9. Lee JW, Samal S, Selvapalam N, Kim HJ, Kim K (2003) Cucurbituril Homologues and Derivatives: New Opportunities in Supramolecular Chemistry. Acc. Chem. Res 36:621-630.
10. Tuncel D, Steinke JHG (2004) Catalytic Self-Threading: A New Route for the Synthesis of Polyrotaxanes. Macromolecules 37:288-302.
11. Carlqvist P, Maseras F (2007) A theoretical analysis of a classic example of supramolecular catalysis. Chem. Commun 748-770.

12. Wheate NJ, Buck DP, Day AI, Collins JG (2006) Cucurbit[n]uril binding of platinum anticancer complexes. Dalton Trans 451-458.
13. Wei F, Liu SM, Xu L, Cheng GZ, Wu CT, Feng YQ (2005) The formation of cucurbit[n]uril (n = 6, 7) complexes with amino compounds in aqueous formic acid studied by capillary electrophoresis. Electrophoresis 26: 2214-2224.
14. Xu L, Liu SM, Wu CT, Feng YQ (2004) Separation of positional isomers by cucurbit[7]uril-mediated capillary electrophoresis, Electrophoresis 25:3300-3306.
15. Rudkevich M (2004) Anti-Markovnikov Hydrofunctionalization of Olefins Mediated by -Rhodium–Porphyrin Complexes. Angew. Chem. Int. Ed 43:558-590.
16. Ong W, Zmez-Kaifer MG, Kaifer AE (2002) Cucurbit[7]uril: A Very Effective Host for Viologens and Their Cation Radicals. Org. Lett 4:1791-174.
17. Ong W, Kaifer AE (2003) Molecular Encapsulation by Cucurbit[7]uril of the Apical 4,4′-Bipyridinium Residue in Newkome-Type Dendrimers. Angew. Chem. Int. Ed 42:2164-2167.
18. Sun S, Zhang R, Andersson S, Pan J, Åkermark B, Sun L (2006) The photoinduced long-lived charge-separated state of Ru(bpy)3–methylviologen with cucurbit[8]uril in aqueous solution. Chem. Commun 4195-4197.
19. Ling Y, Mague JT, Kaifer AE (2007) Inclusion Complexation of Diquat and Paraquat by the Hosts Cucurbit[7]uril and Cucurbit[8]uril. Chem. Eur. J 13:7908-7914.
20. Wagner D, Stojanovic N, Day AI, Blanch RJ (2003) Host Properties of Cucurbit[7]uril: Fluorescence Enhancement of Anilinonaphthalene Sulfonates. J. Phys. Chem. B 107: 10741-10746.
21. Mock WL, Shih NY (1983) Host-guest binding capacity of cucurbituril . J. Org. Chem 48:3618-3619.
22. Lagona J, Mukhopadhyay P, Chakrabarti S, Isaacs L (2005) The Cucurbit[*n*]uril Family. Angew. Chem. Int. Edn 44:4844-4870.
23. Buschmann HJ, Jansen K, Schollmeyer E (2003) Cucurbit[6]uril as ligand for the complexation of lanthanide cations in aqueous solution. Inorg. Chem. Commun 6:531-534.
24. Bali MS, Buck DP, Coe AJ, Day AI, Collins JG (2006) Cucurbituril binding of trans-[{PtCl(NH3)2}2(μ-NH2(CH2)8NH2)]2+ and the effect on the reaction with cysteine. Dalton Trans 5337-5344.

25. Jeon WS, Moon K, Park SH, Chun H, Ko YH, Lee JY, Lee ES, Samal S, Selvapalam N, Rekharsky MV, Sindelar V, Sobransingh D, Inoue Y, Kaifer AE, Kim K (2005) Complexation of Ferrocene Derivatives by the Cucurbit[7]uril Host: A Comparative Study of the Cucurbituril and Cyclodextrin Host Families. J. Am. Chem. Soc 127:12984-12989.
26. Sobransingh D, Kaifer AE (2006) New Dendrimers Containing a Single Cobaltocenium Unit Covalently Attached to the Apical Position of Newkome Dendrons: Electrochemistry and Guest Binding Interactions with Cucurbit[7]uril. Langmuir 22:10540-10544.
27. Zou D, Andersson S, Zhang R, Sun S, Åkermark B, Sun L (2008) A Host-Induced Intramolecular Charge-Transfer Complex and Light-Driven Radical Cation Formation of a Molecular Triad with Cucurbit[8]uril. J. Org. Chem 73:3775-3783.
28. Park KM, Kim SY, Heo J, Whang D, Sakamoto S, Yamaguchi K, Kim K (2002) Designed Self-Assembly of Molecular Necklaces. J. Am. Chem. Soc 124:214021-2104047.
29. Sindelar V, Silvi S, Kaifer AE (2006) Switching a molecular shuttle on and off: simple, pH-controlled pseudorotaxanes based on cucurbit[7]uril, Chem. Commun 2185-2187.
30. Chakraborty A, Wu A, Witt D, Lagona J, Fettinger JC, Isaacs L (2002) Diastereoselective Formation of Glycoluril Dimers: Isomerization Mechanism and Implications for Cucurbit[n]uril Synthesis. J. Am. Chem Soc. 124:8297-8306.
31. Kim J, Jung IS, Kim SY, Lee E, Kang JK, Sakamoto S, Yamaguchi K, Kim K (2000) New Cucurbituril Homologues: Syntheses, Isolation, Characterization, and X-ray Crystal Structures of Cucurbit[n]uril (n = 5, 7, and 8). J. Am. Chem. Soc 122:540-541.
32. Day AI, Arnold AP, Blanch RJ, Snushall B (2001) Controlling Factors in the Synthesis of Cucurbituril and Its Homologues. J. Org. Chem 66:8094-8100.
33. Mock WL (1995) Curubituril, Supramolecular Chemistry II – Host Design and Molecular Recognition. Springer: Berlin/Heidelberg Germany, p 1.
34. Eric M, Xiaoxi L, Roymon J, Lawrence K-M and Xiaoyong L (2012) Cucurbituril chemistry: a tale of supramolecular success. RSC Advances 2:1213–1247.
35. Derick L and Lyle I (2011) Recognition Properties of Acyclic Glycoluril Oligomers. Org. Lett 13: 4112–4115.
36. Lyle I (2009) Cucurbit[n]urils: from mechanism to structure and function. Chem. Commun. 619.

37. Pichierri F (2005) Nanosoldering of thia-cucurbituril macrocycles with transition metals affords novel tubular nanostructures: A computational study. Chem. Phys. Lett 403:252-256.
38. Pinjari RV, Gejji SP (2010) On the Binding of SF6 to Cucurbit[6]uril Host: Density Functional Investigations. J. Phy. Chem. A 114:2338-2343.
39. Pinjari RV, Khedkar JK, Gejji SP (2010) Cavity diameter and height of cyclodextrins and cucurbit[n]urils from the molecular electrostatic potential topography.J. Incl. Phenom. Macrocycl. Chem 66:371-380.
40. Zhang H, Ferrell TA, Asplund MC, Dearden DV (2007) Molecular beads on a charged molecular string: α,ω-alkyldiammonium complexes of cucurbit[6]uril in the gas phase. Int. J. Mass Spectrom 265:187-196.
41. Buschmann HJ, Wego A, Zielesny A, Schollmeyer E (2006) Structure, Stability, Electronic Properties and NMR-Shielding of the Cucurbit[6]uril–Spermine-Complex. J. Inclusion Phenom. Macrocyclic Chem 54:241-246.
42. Pichierri F (2006) DFT study of cucurbit[n]uril, n=5–10. J. Mole. Struct (THEOCHEM) 765 :151-152.
43. Dearden DV, Ferrell TA, Asplund MC, Zilch LW, Julian RR, Jarrold MF (2009) One Ring to Bind Them All: Shape-Selective Complexation of Phenylenediamine Isomers with Cucurbit[6]uril in the Gas Phase. J. Phys. Chem A. 113:989-997.
44. Pinjari RV, Gejji SP (2009) Inverted Cucurbit[n]urils: Density Functional Investigations on the Electronic Structure, Electrostatic Potential, and NMR Chemical Shifts. J. Phy. Chem. A 113:1368-1376.
45. Mock WL, Shih NY (1986) Structure and selectivity in host-guest complexes of cucurbituril. J. Org. Chem 51:4440-4446.
46. Moghaddam S, Yang C, Rekharsky M, Ko YH, Kim K, Inoue Y, Gilson MK (2011) New Ultrahigh Affinity Host-Guest Complexes of Cucurbit[7]uril with Bicyclo[2.2.2] octane and Adamantane Guests: Thermodynamic Analysis and Evaluation of M2 Affinity Calculation. J. Am. Chem. Soc 133:3570-3581.
47. Rekharsky MV, Mori T, Yang C, Ko YH, Selvapalam N, Kim H, Sobransingh D, Kaifer A E, Liu S, Isaacs L et al. (2007) A Synthetic Host-Guest System Achieves Avidin-Biotin

Affinity by overcoming Enthalpy-Entropy Compensation. Proc. Natl. Acad. Sci. U.S.A 104:20737-20742.

48. Chakraborty A, Wu A, Witt D, Lagona J, Fettinger JC, Isaacs L (2002) Diastereoselective Formation of Glycoluril Dimers: Isomerization Mechanism and Implications for Cucurbit[n]uril Synthesis. J. Am. Chem. Soc 124:8297-8306.
49. Wu A, Chakraborty A, Witt D, Lagona J, Damkaci F, Ofori MA, Chiles JK, Fettinger JC, Isaacs L (2002) Methylene-Bridged Glycoluril Dimers: Synthetic Methods. J. Org. Chem 67:5817-5830.
50. Isaacs L, Park SK, Liu S, Ko YH, Selvapalam N, Kim Y, Kim H, Zavalij PY, Kim GH, Lee HS, Kim K (2005) The Inverted Cucurbit[n]uril Family. J. Am. Chem. Soc 127: 18000-18001.
51. Spath A, Konig B (2010) Molecular recognition of organic ammonium ions in solution using synthetic receptors. Beilstein J. Org. Chem 6:32
52. Becke AD (1988) Density-function exchange-energy approximation with correct asymptotic behavior. Phys. Rev. A 38: 3098-3100.
53. Grimme S (2006) Semiempirical GGA-type density functional constructed with a long-range dispersion correction. J. Comp. Chem 27:1787-99.
54. Frisch MJ, Trucks GW, Schlegel HB, Scuseria GE, Robb MA, Cheeseman JRG, Calmani V, Barone B, Mennucci GA, Petersson H, Nakatsuji M, Caricato Li X, Hratchian HP, Izmaylov AF, Bloino J, Zheng G, Sonnenberg JL, Hada M, Ehara M, Toyota K, Fukuda R, Hasegawa J, Ishida M, Nakajima T, Honda Y, Kitao O, Nakai H, Vreven T, Montgomery JA, Peralta Jr JEF, Ogliaro M, Bearpark JJ, Heyd E, Brothers KN, Kudin VN, Staroverov R, Kobayashi J, Normand K, Raghavachari A, Rendell JC, Burant SS, Iyengar J, Tomasi M, Cossi N, Rega JM, Millam M, Klene JE, Knox JB, Cross V, Bakken C, Adamo J, Jaramillo R, Gomperts RE, Stratmann O, Yazyev AJ, Austin R, Cammi C, Pomelli JW, Ochterski RL, Martin K, Morokuma VG, Zakrzewski GA, Voth P, Salvador JJ, Dannenberg S, Dapprich AD, Daniels O, Farkas JB, Foresman JV, Ortiz J, Cioslowski Fox DJ (2009) Gaussian, Inc., Wallingford CT, Gaussian 09, Revision A 02.
55. Yan Z, Donald G.T (2007) The M06 suite of density functionals for main group thermochemistry, thermochemical kinetics, noncovalent interactions, excited states, and

transition elements: two new functionals and systematic testing of four M06-class functionals and 12 other functionals. Theor Chem Account. 120:215–241

56. Frischet M.J. al., Gaussian, (2010) Inc., Wallingford, CT, GAUSSVIEW, under Gaussian 09.

57. Bader RFW (1990) In Atoms in molecules: A Quantum Theory; Oxford University Press; Clarendon, Koch U, Popelier PLA (1995) Characterization of C-H-O Hydrogen Bonds on the Basis of the Charge Density. J. Phys Chem 99:9747-9754.

58. Popelier PLA (1998) Characterization of a Dihydrogen Bond on the Basis of the Electron Density. J. Phys. Chem. A 102:1873-1878.
59. Limaye AC, Gadre SR (2001) UNIVIS-2000: An indigenously developed comprehensive visualization package. Curr. Sci 80:1298-1301.
60. Wolinski K, Hilton JF, Pulay P (1990) Efficient implementation of the gauge-independent atomic orbital method for NMR chemical shift calculations. J. Am. Chem. Soc 112:8251-8260.
61. Miertus S, Scrocco E, Tomasi J (1981) Electrostatic interaction of a solute with a continuum. A direct utilizaion of AB initio molecular potentials for the prevision of solvent effects. Chem. Phys 55:117-129.

Table 1 Comparison of (**a**) B97D/6-31G(d,p), (**b**) B97D/6-31+G(d,p) and (**c**) B97D/6-31++G(d,p) energies of inclusion complexes. .

	CB[6] ΔE_{Bind}			**CB[7]** ΔE_{Bind}			**iCB[6]** ΔE_{Bind}			**iCB[7]** ΔE_{Bind}		
	a	**b**	**c**	**a**	**b**	**c**	**a**	**b**	**c**	**a**	**b**	**c**
HDA	704.5	651.7	651.5	682.0	634.3	632.9	622.3	569.3	564.7	642.9	590.9	589.9
XYL	752.5	696.3	695.8	717.9	671.9	672.4	685.8	631.2	629.8	677.4	629.8	628.5

Table 2 B97D/6-31+G(d,p) energies of the Complexes of HDA and XYL with CB[n] and *i*CB[n] and the energy in water (SCRF-PCM) are given in parentheses.

	CB[6]		CB[7]		iCB[6]		iCB[7]	
	ΔE_{Rel}	ΔE_{Bind}	ΔE_{Rel}	ΔE_{Bind}	ΔE_{Rel}	ΔE_{Bind}	ΔE_{Rel}	ΔE_{Bind}
HDA								
A	0.0 (0.0)	651.7(220.9)	0.0 (0.0)	634.3(192.9)	0.0(0.0)	569.0(187.5)	0.0(0.0)	590.9(190.2)
B			5.5(1.2)	628.8(191.8)			4.2(4.5)	586.8(185.7)
C	9.7(18.9)	642.0(202.0)	11.9(7.9)	622.4(185.1)	8.0(3.4)	561.0(184.1)	21.1(17.9)	569.8(172.3)
XYL								
A	0.0 (0.0)	696.3(229.2)	0.0 (0.0)	671.9(201.9)	0.0(0.0)	631.3(214.6)	0.0 (0.0)	629.8(198.1)
B	9.9(3.9)	686.4(225.3)						
C			3.2(9.2)	668.7(192.7)	9.2(0.8)	622.1(213.8)	2.3(5.9)	627.4(192.3)

Table 3 The hydrogen bonded distances (in Å) and ρ_{bcp} (in au) in the minimum energy host-guest complexes.

	CB[6]-XYL-A		CB[7]-XYL-A		iCB[6]-XYL-A		iCB[7]-XYL-A		CB[6]-HDA-A		CB[7]-HDA-A		iCB[6]-HDA-A		iCB[7]-HDA-A	
	Dist	ρ_{bcp}	Dist	ρ_{bcp}	Dist	ρ_{bcp}	Dist	ρ_{bcp}	Dist	ρ_{bcp}	Dist	ρ_{bcp}	Dist	ρ_{bcp}	Dist	ρ_{bcp}
N-H---O	2.079	0.0184	1.841	0.0309	1.894	0.0269	1.922	0.0256	1.983	0.0228	1.877	0.0279	1.738	0.0407	1.857	0.0295
	2.198	0.0154	1.847	0.0305	2.377	0.0122	2.414	0.0110	1.950	0.0253	2.477	0.0104	1.974	0.0241	1.912	0.0273
	1.861	0.0289	1.881	0.0279	1.909	0.0263	1.859	0.0291	1.981	0.0229	1.924	0.0265	2.388	0.0125	2.452	0.0106
	2.382	0.0099	2.492	0.0102	1.957	0.0238	1.973	0.0226	2.357	0.0131	1.904	0.0279	1.963	0.0235	1.912	0.0265
	1.996	0.0224	1.893	0.0272	2.298	0.0136	1.867	0.0291	1.953	0.0251	2.408	0.0112	2.376	0.0125	2.432	0.0109
	1.821	0.0318			1.864	0.0288	2.502	0.0104			1.955	0.0238			1.865	0.0303
C-H---O	2.311	0.0121			2.260	0.0133	2.333	0.0128	2.275	0.0132			2.449	0.0091		
	2.238	0.0139			2.229	0.0142			2.273	0.0132			2.417	0.0106		
					2.507	0.0105							2.183	0.0162		

Table 4 Vibrational frequencies in the CB[n], *i*CB[n] hosts, HDA and their minimum energy complexes. *The frequeincies are scaled by 0.9766 as reported in Ref. bull.chem.soc.jpn . 2012 ,85(9) , pp.962-975**.** [a]Vibrational modes corresponds to inverted glycouril unit.

	HDA	CB[6]	CB[6] HDA -A	CB[7]	CB[7] HDA -A	*i*CB[6]	*i*CB[6]HDA-A	*i*CB[7]	*i*CB[7]HDA-A
ν (C-H1)				2989(2)	3011(1) 2998(4)	2991(1) 2982(2)	3006(3) 2997(2)	2997(1) 2990(2)	3010(2) 2996(3)
ν (C-H2)		2894(150) 2892(142) 2876(311) 2838(81)	2918(120) 2916(73) 2913(69)	2878(122) 2877(93) 2876(111) 2861(257) 2860(242)	2921(88) 2919(47) 2915(62)	2897(139) 2895(69) 2886(93) 2880(171)	2919(37) 2913(65) 2900(38)	2989(4) 2893(127) 2892(101) 2875(97) 2862(336) 2858(266)	2926(84) 2918(53) 2917(45) 2869(33)
ν (C-H3)		2858(328) 2857(279) 2847(34)	2907(26) 2905(77) 2900(83)	2856(117) 2855(73) 2854(80) 2851(107)	2896(130) 2911(95)	2964(31) 2896(150) 2863(105) 2858(92)	2967(46) 2942(63) 2905(57)	2966(30) 2852(34)	2995(20) 2963(30) 2941(37) 2923(75)
ν (C-O)		1782(2525) 1775(127) 1774(153)	1766(1527) 1751(279) 1747(786) 1740(162) 1710(122) 1707(106) 1704(197)	1777(3087) 1774(178) 1765(176)	1784(192) 1781(935) 1761(211) 1756(210) 1745(394) 1741(986) 1735(184) 1730(170) 1709(205) 1701(142) 1698(109) 1691(220)	1779(1921) 1773(441) 1767(89) 1740(257) 1749(36)[a] 1733(272)	1770(419) 1761(782)[a] 1752(388) 1749(517) 1743(401) 1736(197) 1713(236) 1702(209)	1776(1862) 1773(1083) 1769(102) 1758(118) 1738(260)[a] 1730(288)	1785(556) 1763(446) 1750(322)[a] 1749(244) 1743(636) 1740(545) 1739(439) 1722(407) 1710(193) 1702(256) 1699(131) 1692(158)
CH_2 sci		1401(269) 1397(515) 1395(561) 1393(114) 1392(229)	1405(299) 1400(70) 1394(129)	1398(276) 1397(494) 1396(336) 1395(168) 1394(183)	1410(474) 1399(107) 1394(128)	1434(70) 1394(108) 1398(135) 1397(379) 1395(303)	1429(121) 1420(251) 1406(148)	1438(92) 1398(711) 1397(138) 1395(133) 1395(200)	1435(66) 1421(340) 1418(337) 1415(126) 1408(84)

Table 4 cont…

HDA	CB[6]	CB[6] HDA-A	CB[7]	CB[7] HDA-A	*i*CB[6]	*i*CB[6] HDA-A	*i*CB[7]	*i*CB[7]HDA-A
CH_2 wag	1386(58) 1283(376)	1415(611) 1395(69) 1337(183) 1184(108) 1181(432)	1341(215) 1277(425)	1335(202) 1332(250) 1330(256) 1288(144) 1285(560) 1282(120)	1396(301) 1395(107) 1366(114) 1352(202) 1345(157) 1341(148) 1283(350) 1288(211) 1280(268) 1276(140) 1269(356)	1414(641) 1355(93) 1347(110) 1335(105) 1287(102) 1281(233) 1278(109) 1274(188)	1398(664) 1370(149) 1354(131) 1352(103) 1337(124) 1331(510) 1292(204) 1272(532) 1269(254)	1412(343) 1401(219) 1393(178) 1342(179) 1336(140) 1334(141) 1333(132) 1295(123) 1285(578) 1275(143) 1272(266) 1149(156) 1138(181)
CH_2 rock			1166(430) 1165(945) 1140(1056)	1172(489) 1150(332) 1147(136) 1142(205) 1141(739)	1172(367) 1169(387) 1168(541) 1140(576) 1136(119)	1212(72) 1185(151) 1183(124) 1182(338) 1140(480)	1169(907) 1168(796) 1167(258) 1137(105) 1122(150)	1205(116) 1185(124) 1175(423) 1143(322) 1136(121)
ν (C-C)	1331(449)	932(52)	1360(473)		1327(183)	1321(20)	1283(70)	
ν (C-N)	1254(422) 1240(152) 1239(189)	1440(18) 1103(33) 1091(19)	1253(300) 1251(168) 1242(118)	1255(102) 1254(100) 1246(126) 1239(124)	1250(180) 1249(93) 1239(130) 1237(101)	1236(158) 1189(197) 1173(143)	1251(134) 1245(289) 1241(104) 1239(131) 1180(136)	1247(95) 1238(54) 1196(62) 1179(194) 1168(299)
ν (C-N)+ δ (C-H)	1118(82)		1206(114)	1210(109)	1183(183)	1143(379) 1198(67)	1231(48) 1206(432)	1232(23) 1221(34)
δ (N-C-N)	635(84)	662(22)	768(421)	768(7)	641(44)	647(8)	764(67)	768(197)

Table 4 cont…

	HDA	CB[6]	CB[6] HDA -A	CB[7]	CB[7] HDA -A	*i*CB[6]	*i*CB[6]HDA-A	*i*CB[7]	*i*CB[7]HDA-A
ν (NH)	3347(182) 3345(208) 3240(107)		3374(171) 3193(612) 3192(232) 3134(150) 3133(139)		3367(80) 3139(573) 3150(583) 3072(283)		3365(106) 3187(436) 3118(148) 3085(292)		3365(89) 3120(709) 3145(682) 3056(491)
ν (CH_2)	3033(3) 2973(43) 2961(6) 2910(46)		3065(5) 3026(10) 2975(34) 2923(22) 2922(16)		3035(125) 3032(2) 2980(19)		3048(13) 2993(20) 2899(37) 2982(24)		3040(11) 2968(29) 2972(28) 2909(17) 2905(23)
δ (NH2)	1602(79) 1601(116)		1608(75) 1606(58) 1453(123)		1608(34) 1464(113) 1460(121)		1616(168) 1610(17) 1590(79)		1603(44) 1601(32)
CH_2 sci	1448(106) 1435(5)		1451(52) 1431(30) 1424(104)		1424(101) 1431(83)		1459(63) 1453(92) 1449(86) 1423(127)		1456(123) 1450(79) 1431(24)
CH_2 wag	1215(7) 1060(57)		1339(68) 1242(59) 1240(194)		1347(8) 1343(17)		1355(5) 1297(8) 1243(102)		1251(31) 1252(25) 1235(17)
CH2 twist	1288(8)		1316(15) 1312(44) 1205(33)		1302(35)		1323(21) 1296(19)		1317(38) 1292(36) 1281(47)
C-C	967(6) 887(9) 814(49)		1326(8) 998(9)		1043(10)		969(3)		989(4) 988(13) 965(17)

Table 5 Vibrational frequencies in the CB[n], *i*CB[n] hosts, XYL and their minimum energy complexes. *The frequeincies are scaled by 0.9766 as reported in Ref. bull.chem.soc.jpn . 2012 ,85(9) , pp.962-975**.** [a]Vibrational modes corresponds to inverted glycouril unit.

XYL	CB[6]	CB[6]-XYL-A	CB[7]	CB[7]-XYL-A	*i*CB[6]	*i*CB[6]-XYL-A	*i*CB[7]	*i*CB[7]-XYL-A
ν (C-H1)		3003(1) 3000(2)	2989(2)	3009(2) 3004(80)	2991(1) 2982(2)	3013(2)	2997(1) 2990(2)	3008(4) 2996(108)
ν (C-H2)	2894(150) 2892(142) 2876(311) 2838(81)	2922(94) 2914(29) 2913(76) 2911(89)	2878(122) 2877(93) 2876(111) 2861(257) 2860(242)	2918(67) 2917(72) 2916(65) 2911(99)	2897(139) 2895(69) 2886(93) 2880(171)	2924(45) 2923(64) 2921(60)	2893(127) 2892(101) 2875(97) 2862(336) 2858(266)	2923(63) 2910(47) 2895(58)
ν (C-H3)	2858(328) 2857(279) 2847(34)	2910(53) 2909(67)	2856(117) 2855(73) 2854(80) 2851(107)	2913(45) 2908(60) 2905(78) 2901(63)	2964(31) 2896(150) 2863(105) 2858(92)	3039(6) 2940(37) 2939(39)	2966(30) 2852(34)	2953(32) 2929(44) 2920(56) 2916(105)
ν (C-O)	1782(2525) 1775(127) 1774(153)	1715(132) 1763(1243) 1748(532) 1737(931)	1777(3087) 1774(178) 1765(176)	1783(393) 1772(885) 1768(249) 1753(386) 1743(577) 1735(262) 1708(431) 1697(105) 1693(229)	1779(1921) 1773(441) 1767(89) 1740(257) 1749(36)[a] 1733(272)	1762(114)[a] 1755(1354) 1745(268) 1738(735) 1736(245) 1728(117) 1712(122) 1697(184) 1696(188)	1776(1862) 1773(1083) 1769(102) 1758(118) 1738(260)[a] 1730(288)	1770(119) 1769(943) 1757(12)[a] 1750(402) 1747(246) 1744(720) 1739(382) 1738(283) 1731(226) 1708(203) 1697(128) 1694(219)
CH_2 sci	1401(269) 1397(515) 1395(561) 1393(114) 1392(229)	1412(546) 1405(189) 1402(62) 1394(106)	1398(276) 1397(494) 1396(336) 1395(168) 1394(183)	1409(229) 1400(310) 1396(92)	1434(70) 1394(108) 1398(135) 1397(379) 1395(303)	1444(82) 1442(98) 1431(62) 1430(112) 1423(367)	1438(92) 1398(711) 1397(138) 1395(133) 1395(200)	1443(70) 1426(197) 1400(131) 1396(113) 1394(135)

Table 5 cont…

	XYL	CB[6]	CB[6]-XYL-A	CB[7]	CB[7]-XYL-A	*i*CB[6]	*i*CB[6]-XYL-A	*i*CB[7]	*i*CB[7]-XYL-A
CH2 wag		1386(58) 1283(376)	1422(914) 1281(500) 1280(376) 1139(630) 1338(269) 1337(248)	1341(215) 1277(425)	1415(518) 1336(160) 1334(260) 1332(261) 1286(215) 1280(254) 1210(130) 1209(206)	1396(301) 1395(107) 1366(114) 1352(202) 1345(157) 1341(148) 1283(350) 1288(211) 1280(268) 1276(140) 1269(356)	1367(82) 1347(96) 1339(253) 1333(118) 1291(141)	1398(664) 1370(149) 1354(131) 1352(103) 1337(124) 1331(510) 1292(204) 1272(532) 1269(254)	1409(142) 1285(185) 1286(367) 1370(105) 1357(136) 1338(128) 1337(127) 1332(161) 1330(159)
CH2 rock				1166(430) 1165(945) 1140(1056)	1170(450) 1171(241) 1142(247) 1141(589) 1140(226) 1139(480)	1172(367) 1169(387) 1168(541) 1140(576) 1136(119)	1206(64) 1183(229) 1140(435) 1139(402) 1137(168)	1169(907) 1168(796) 1167(258) 1137(105) 1122(150)	1180(353) 1172(178) 1169(329) 1170(190) 1141(522) 1137(488)
ν (C-C)		1331(449)	1332(14)	1360(473)		1327(183)	1329(21)	1283(70)	
ν (C-N)		1254(422) 1240(152) 1239(189)	1442(79) 1242(289) 1237(136) 1235(134)	1253(300) 1251(168) 1242(118)	1427(165) 1256(103) 1252(143)	1250(180) 1249(93) 1239(130) 1237(101)	1233(133)	1251(134) 1245(289) 1241(104) 1239(131) 1180(136)	1247(129) 1242(26) 1205(42) 1204(70)
ν (C-N)+ δ (C-H)		1118(82)	1249(61) 1242(289)	1206(114)	1234(31)	1183(183)	1235(131)	1231(48) 1206(432)	1231(31) 1208(125)
δ (N-C-N)		635(84)	647(112)	768(421)	780(283)	641(44)	648(41) 646(80)	764(67)	767(255)

Table 5 cont….

	XYL	**CB[6]**	**CB[6]-XYL-A**	**CB[7]**	**CB[7]-XYL-A**	***i*CB[6]**	***i*CB[6]-XYL-A**	***i*CB[7]**	***i*CB[7]-XYL-A**
ν (NH)	3354(160) 3339(150) 3205(247)		3381(110) 3150(277) 3059(450) 3053(303)		3360(72) 3120(748) 3092(748) 3003(496)		3369(107) 3149(473) 3105(535) 3047(354)		3366(94) 3150(582) 3105(455) 3043(290)
ν (CH)	3054(3)		3146(3)		3098(8)		3168(3)		3063(8)
ν (CH2)	2966(1)		3045(16)		3047(37)		3041(3)		3034(64)
δ (NH2)	1599(65) 1595(124) 1440(207)		1622(38) 1607(191) 1606(74) 1489(294)		1623(115) 1611(70) 1496(248) 1467(110)		1599(77) 1598(43) 1458(142) 1460(72)		1635(48) 1628(54)
CH2 sci	1431(15)		1420(91)		1442(9)		1418(210) 1418(613) 1410(132)		1448(5) 1421(37)
CH2 wag	1387(12) 1335(122)		1403(13)		1480(3) 1343(60)		1398(52) 1299(43)		1327(10) 1187(10)
CH2 twist	1258(8)				1306(6) 1273(22)		1284(58)		1296(22)
C-C	1319(12) 1169(38)		1499(34)		1327(1)		1314(5)		1310(6) 1166(3)

Table 6 Electron density in anti-bonding orbital (σ* in au), Bond Distances (r in Å), and frequency of vibration (ν in cm^{-1}) in host and their complexes.

					CB[6]-HDA-A			CB[7]-HDA-A			*i*CB[6]-HDA-A			*i*CB[7]-HDA-A		
		σ*	r	ν	σ*	r	ν	σ*	r	ν	σ*	r	ν	σ*	r	ν
CB[6]	C=O	0.2370	1.218	1777	0.3979	1.223	1755									
CB[7]		0.2032	1.219	1772				0.3804	1.225	1751						
iCB[6]		0.3644	1.224	1758							0.4254	1.238	1746			
iCB[7]		0.2637	1.218	1757										0.3881	1.235	1739
HDA	N-H	0.0054	1.030	3240	0.0410	1.039	3193	0.0455	1.038	3150	0.0407	1.036	3187	0.0514	1.042	3145

					CB[6]-XYL-A			CB[7]-XYL-A			*i*CB[6]-XYL-A			*i*CB[7]-XYL-A		
		σ*	r	ν	σ*	r	ν	σ*	r	ν	σ*	r	ν	σ*	r	ν
CB[6]	C=O	0.2380	1.218	1777	0.4160	1.233	1741									
CB[7]		0.2172	1.218	1772				0.3987	1.228	1759						
iCB[6]		0.2513	1.218	1758							0.3959	1.231	1747			
iCB[7]		0.2185	1.219	1757										0.3978	1.232	1745
XYL	N-H	0.0077	1.029	3205	0.0484	1.042	3150	0.0497	1.042	3120	0.0481	1.040	3149	0.0424	1.038	3150

Table 7 NMR chemical shifts of host protons in the host-guest complexes and chemical shifts in water (SCRF-PCM) are given in parentheses.

		Host			HDA- Complex			XYL-Complex		
		H1	H2	H3	H1	H2	H3	H1	H2	H3
CB[6]		6.1-6.3	3.2-3.5	4.7-4.8	5.9-6.3	3.7-3.8	4.8-5.0	5.8-6.4	3.4-3.7	4.9-5.6
		(5.6-5.8)	(3.7-4.0)	(5.0-5.1)	(5.6-6.0)	(3.9-4.1)	(5.0-5.1)	(5.5-6.0)	(3.7-4.0)	(5.0-5.5)
iCB[6]	*i*			4.3-4.5			4.2-5.1			3.5-3.6
				(4.8-5.0)			(4.6-5.0)			(3.9-4.0)
	α	5.6-6.0	3.7-4.1	4.8-5.1	5.6-5.9	4.2-4.3	5.1-5.3	5.4-5.6	3.6-4.0	5.0-5.3
		(5.4-5.6)	(4.0-4.3)	(5.2-5.4)	(5.4-5.8)	(4.3-4.6)	(5.3-5.5)	(5.1-5.3)	(3.7-4.1)	(5.2-5.6)
	β	6.2-6.3	3.3-3.5	4.7-4.8	6.0-6.1	3.6-3.9	5.1-5.3	6.3-6.5	4.0-4.1	4.8-5.1
		(5.7-5.9)	(3.7-4.1)	(4.9-5.1)	(5.6-5.8)	(3.7-4.1)	(5.2-5.5)	(6.0-6.2)	(4.3-4.4)	(4.9-5.3)
	γ	6.2-6.4	3.3-3.4	4.7-4.7	5.9-6.3	3.5-3.7	4.9-4.9	5.9-6.1	3.5-3.8	4.6-4.7
		(5.7-5.9)	(3.8-3.9)	(5.1)	(5.7-5.8)	(3.8-4.1)	(5.2)	(5.6-5.8)	(3.8-4.0)	(4.7-4..8)
iCB[7]	*i*			4.7-4.8			4.2-4.6			3.5-4.3
				(4.9-5.0)			(4.5-4.8)			(3.6-4.4)
	α	5.7-5.9	3.6-4.1	4.6-4.9	5.5-6.0	3.7-4.4	4.7-5.1	5.1-6.0	3.8-4.2	4.8-5.1
		(5.4-5.6)	(3.8-4.3)	(4.9-5.2)	(5.4-5.6)	(3.9-4.4)	(5.0-5.2)	(5.1-5.6)	(3.9-4.3)	(5.1-5.2)
	β	6.3	3.3-3.5	4.6-4.9	5.7-6.2	3.6-3.8	4.7-4.9	6.0-6.4	3.7-3.9	4.8-5.0
		(5.7-5.8)	(3.8-4.0)	(5.1-5.3)	(5.7-5.9)	(3.9-4.1)	(5.0-5.2)	(5.7-6.0)	(4.0-4.2)	(5.1-5.2)
	γ	6.3-6.4	3.3-3.4	4.6-4.8	5.9-6.2	3.5-3.8	4.8-5.1	5.8-6.4	3.5-4.0	4.8-5.0
		(5.7-5.8)	(3.8-4.0)	(5.0-5.2)	(5.5-5.8)	(3.9-4.0)	(5.0-5.3)	(5.6-6.1)	(3.8-4.4)	(5.1-5.2)
	δ	6.2-6.4	3.3-3.4		5.9	3.5-4.0		5.8-6.0	3.4-3.6	
		(5.6-5.8)	(3.8-3.9)		(5.6-5.7)	(3.9-4.3)		(5.7)	(3.8-3.9)	
CB[7]		6.2-6.4	3.1-3.5	4.5-4.8	5.8-6.3	3.4-3.9	4.6-5.1	5.6-6.3	3.3-3.9	4.7-5.0
		(5.6-5.9)	(3.7-4.0)	(4.9-5.3)	(5.6-5.9)	(3.7-4.2)	(4.9-5.2)	(5.4-5.9)	(3.7-4.1)	(4.9-5.3)

Table 8 NMR chemical shifts of the guest protons in the *Host*-XYL and *Host*-HDA complexes* and chemical shifts in water (SCRF-PCM) are given in parentheses.

XYL	CB[6]-XYL-A	CB[7]-XYL-A	*i*CB[6]-XYL-A	*i*CB[7]-XYL-A	HDA	CB6-HDA-A	CB7-HDA-A	*i*CB6-HDA-A	*i*CB7-HDA-A
N-H					**N-H**				
4.2(4.4)	3.8(4.0)	3.7(4.0)	3.9(4.4)	3.8(4.1)	**4.2(4.6)**	**6.6(6.8)**	**6.7(5.7)**	**6.5(7.1)**	**7.6(6.3)**
4.2(4.8)	**7.7(6.5)**	**7.4(7.3)**	**8.3(7.5)**	**7.3(6.2)**	4.7(4.3)	3.6(6.3)	3.5(3.8)	3.6(3.7)	3.5(3.8)
4.2(4.4)	**6.7(7.9)**	**7.4(7.5)**	**7.3(7.5)**	**6.5(6.9)**	**4.2(4.3)**	**6.4(6.8)**	**6.6(7.0)**	**6.6(5.8)**	**6.7(7.0)**
4.2(4.4)	3.7(4.1)	3.7(4.1)	4.0(4.4)	3.9(4.3)	4.7(4.3)	3.6(3.8)	3.5(3.9)	3.4(3.8)	3.5(3.8)
4.2(4.8)	**6.8(7.7)**	**7.2(6.9)**	**7.8(7.6)**	**7.8(6.9)**	**4.2(4.6)**	**6.4(6.8)**	**6.6(6.8)**	**5.8(4.8)**	**7.0(7.3)**
4.2(4.4)	**7.8(6.5)**	**7.2(6.9)**	**8.2(7.7)**	**7.7(7.9)**	**4.2(4.3)**	**6.6(6.3)**	**7.2(6.6)**	**8.6(9.2)**	**6.9(6.1)**
C-H (methylene)					**C-H (methylene)**				
4.6(4.4)	**5.0(4.7)**	4.4(4.1)	4.1(3.9)	3.9(3.7)	3.5(3.3)	3.6(3.0)	3.3(3.1)	2.3(2.0)	2.8(2.6)
4.6(4.4)	**4.9(4.6)**	4.2(3.9)	**5.3(4.9)**	4.6(4.1)	3.5(3.3)	3.5(3.1)	3.1(2.5)	3.2(2.7)	3.7(3.3)
4.6(4.4)	**4.8(4.5)**	4.3(4.0)	4.2(4.0)	**5.3(5.2)**	1.9(1.7)	0.2(0.3)	0.3(0.5)	0.7(0.6)	0.6(0.7)
4.6(4.4)	**5.0(4.7)**	4.6(4.3)	**5.4(5.0)**	4.1(4.0)	1.9(1.7)	0.6(0.8)	1.1(1.2)	0.6(0.8)	1.0(1.3)
C-H (aromatic)					1.7(1.5)	1.0(0.8)	1.1(1.1)	0.1(0.1)	0.9(0.8)
8.0(7.7)	6.5(6.5)	7.0(6.9)	7.2(7.1)	7.0(6.9)	1.7(1.5)	0.4(0.5)	0.5(0.4)	1.7(0.7)	1.0(0.9)
8.0(7.7)	7.0(7.0)	7.3(7.3)	7.2(7.0)	7.2(7.1)	1.7(1.5)	1.0(0.8)	1.3(0.9)	0.6(0.6)	1.2(1.2)
8.0(7.7)	7.1(6.9)	7.0(7.0)	6.5(6.6)	7.5(7.4)	1.7(1.5)	0.4(0.5)	0.6(0.5)	1.2(0.6)	0.4(0.5)
8.0(7.7)	6.8(6.6)	7.2(7.3)	7.0(6.9)	6.5(6.6)	1.9(1.7)	0.2(0.3)	0.5(0.5)	0.9(0.8)	0.4(0.6)
					1.9(1.7)	0.6(0.8)	1.0(1.2)	0.2(0.1)	1.0(1.2)
					3.5(3.3)	3.6(3.0)	3.4(2.8)	3.5(3.1)	3.5(3.2)
					3.5(3.3)	3.5(3.1)	3.3(3.0)	3.3(2.7)	3.1(2.7)

* The values shown in bold are corresponds to the protons participating in the hydrogen bonding with ureido oxygens in CB[n]/iCB[n] portals.

Figure Captions

Fig. 1 (a) Cucurbit[7]uril and (b) inverted diastereomer iCB[7].

Fig. 2 Optimized structures of HDA, XYL, and *i*CB monomer.

Fig. 3 MED critical points in the hydrogen bonding interactions in lowest energy complexes.

Fig. 4 ^{1}H NMR chemical shifts for (a) **guest** protons (b) **host** protons in the complexes.

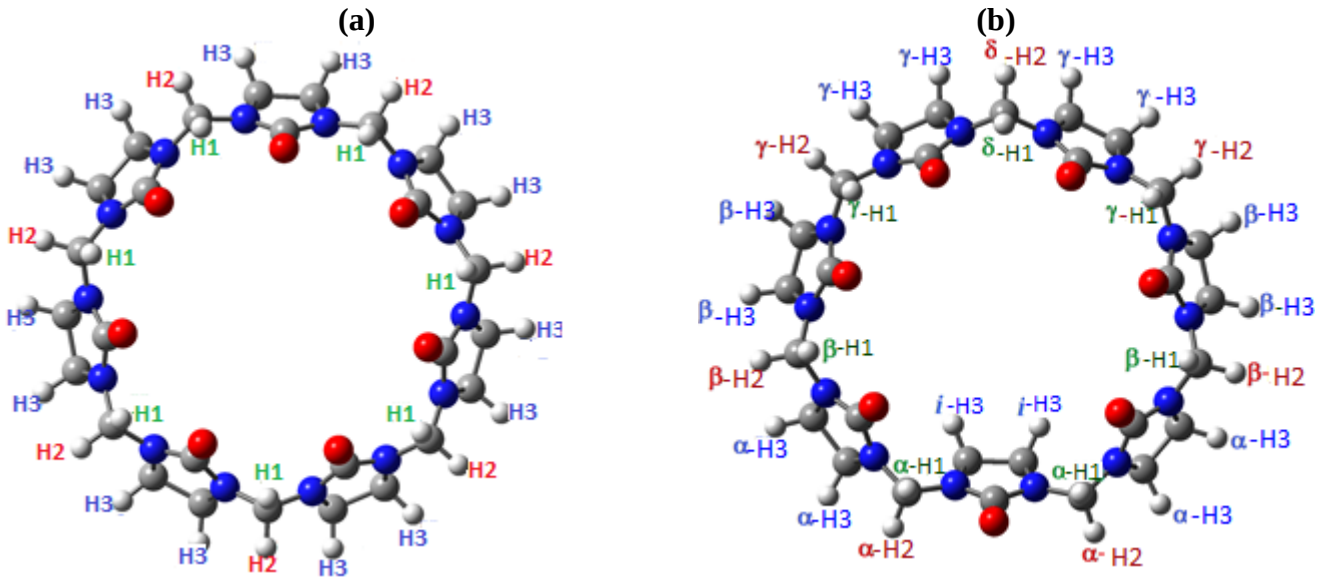

Fig. 1

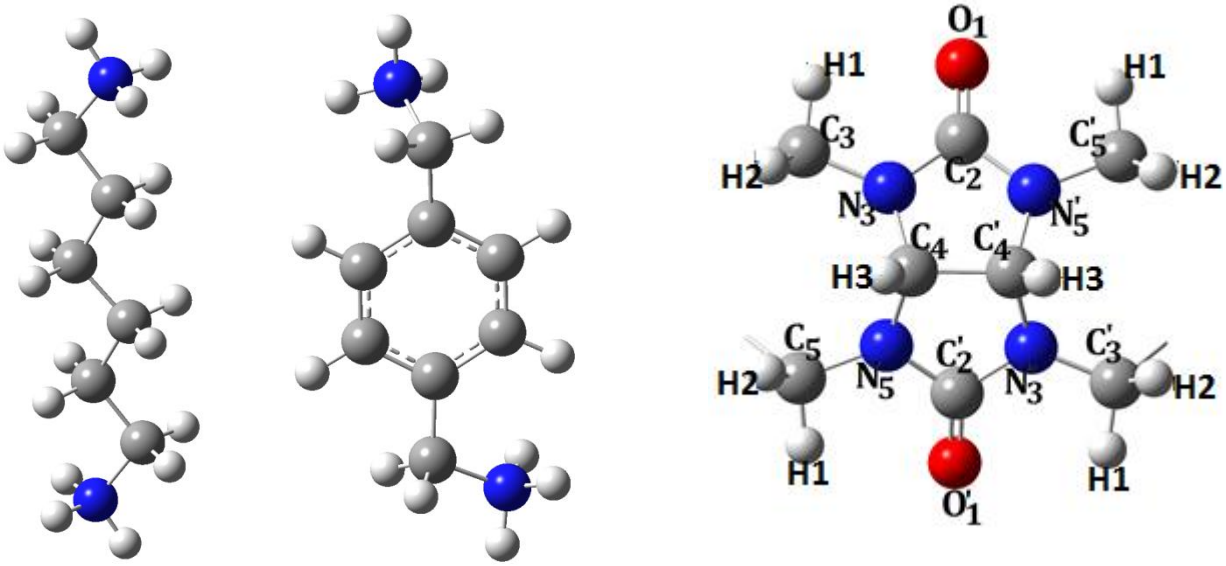

HDA XYL monomer

Fig. 2

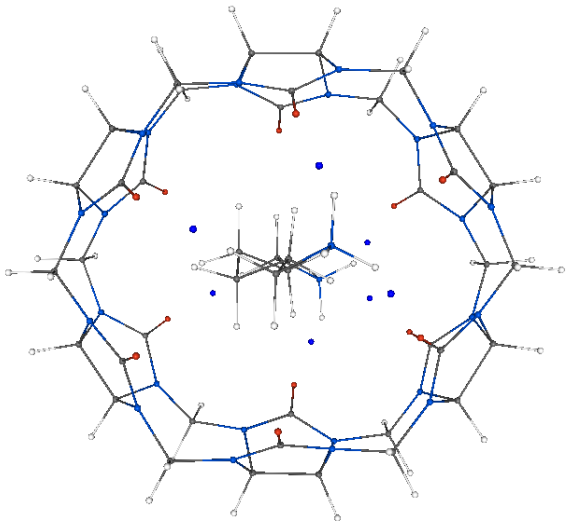

CB[6]-HDA-A

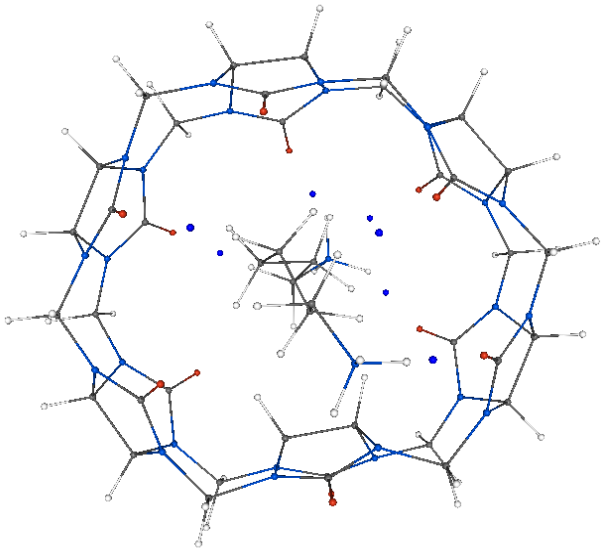

iCB[6]-HDA-A

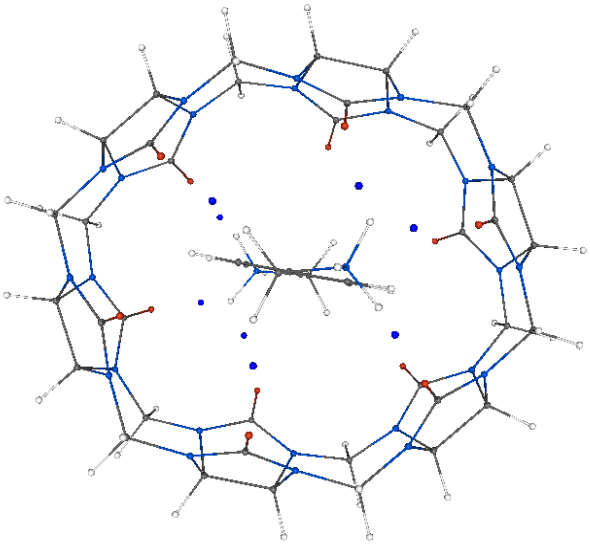

CB[6]-XYL-A

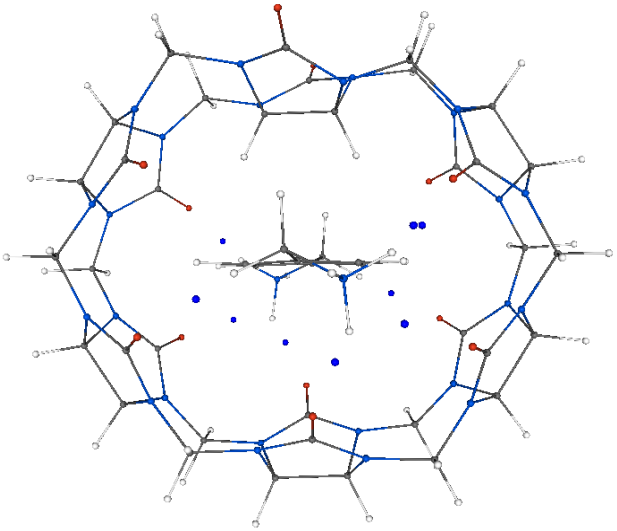

iCB[6]-XYL-A

Fig. 3(a)

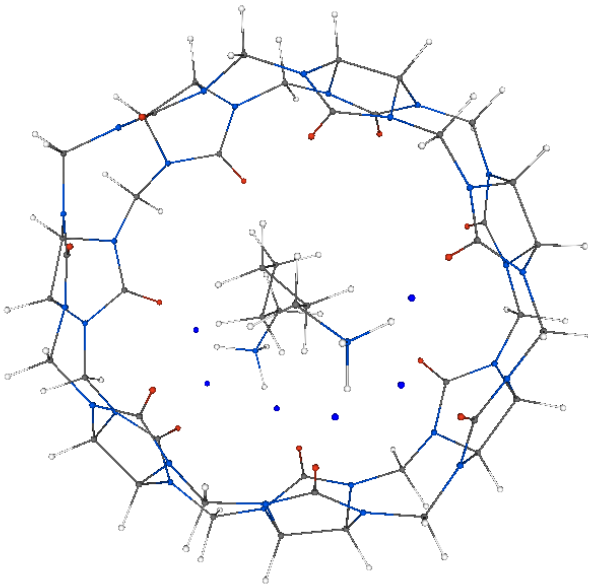

CB[7]-HDA-A

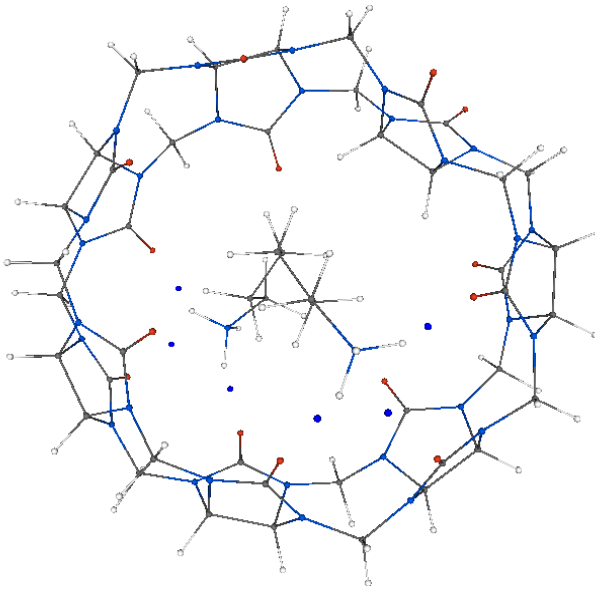

iCB[7]-HDA-A

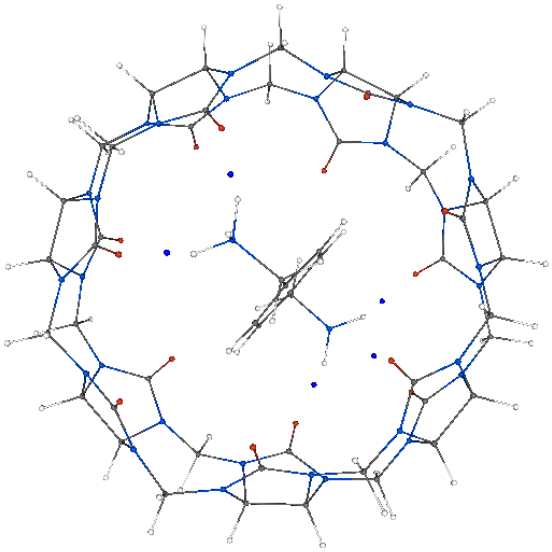

CB[7]-XYL-A

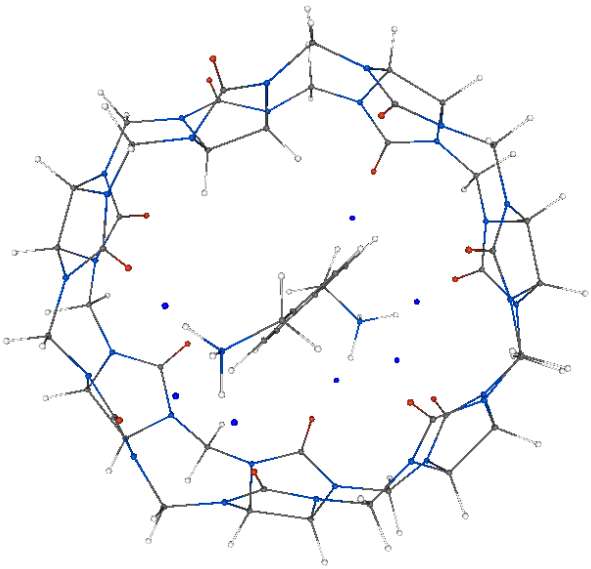

iCB[7]-XYL-A

Fig. 3(b)

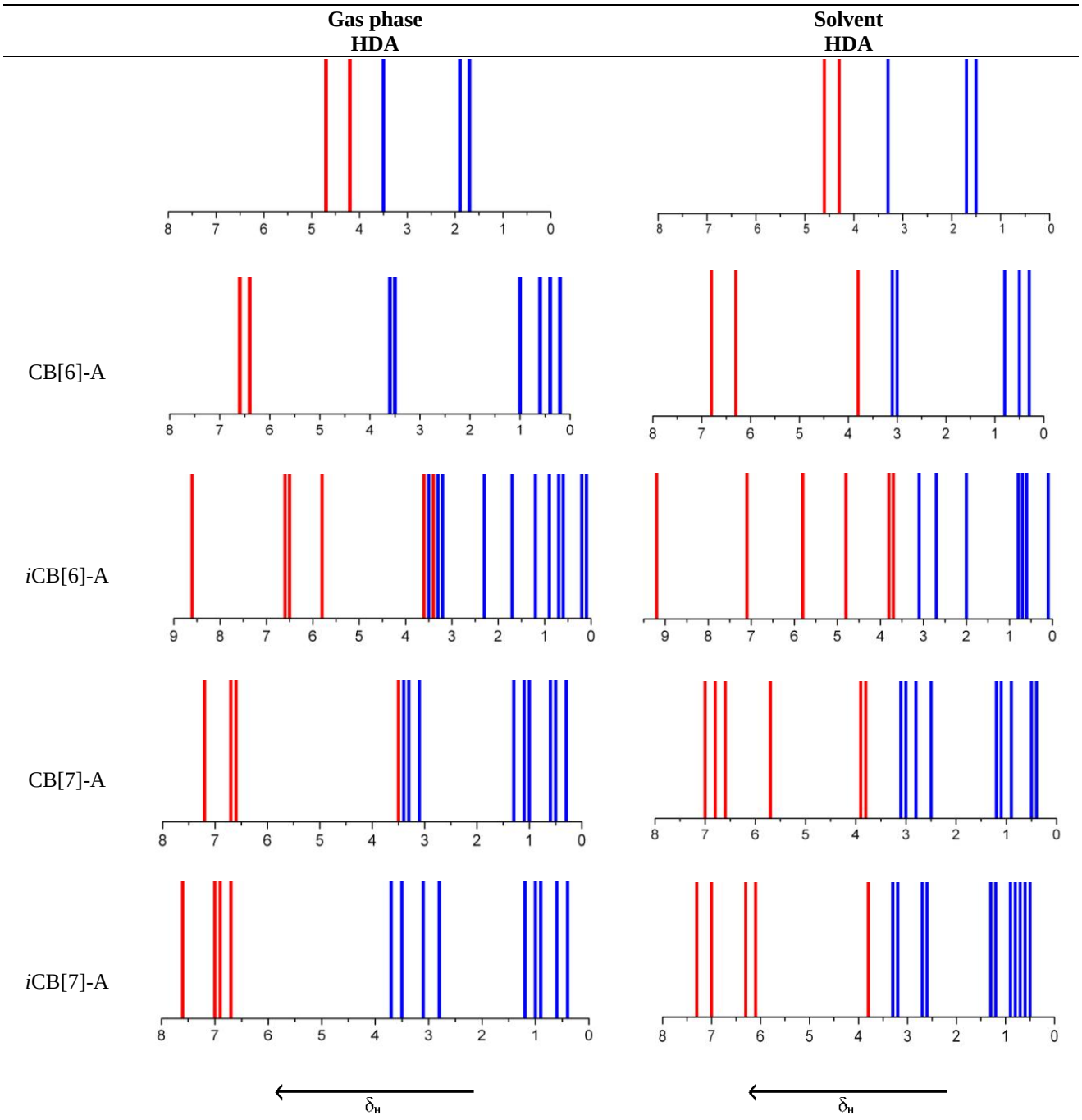

Fig. 4(a) cont...

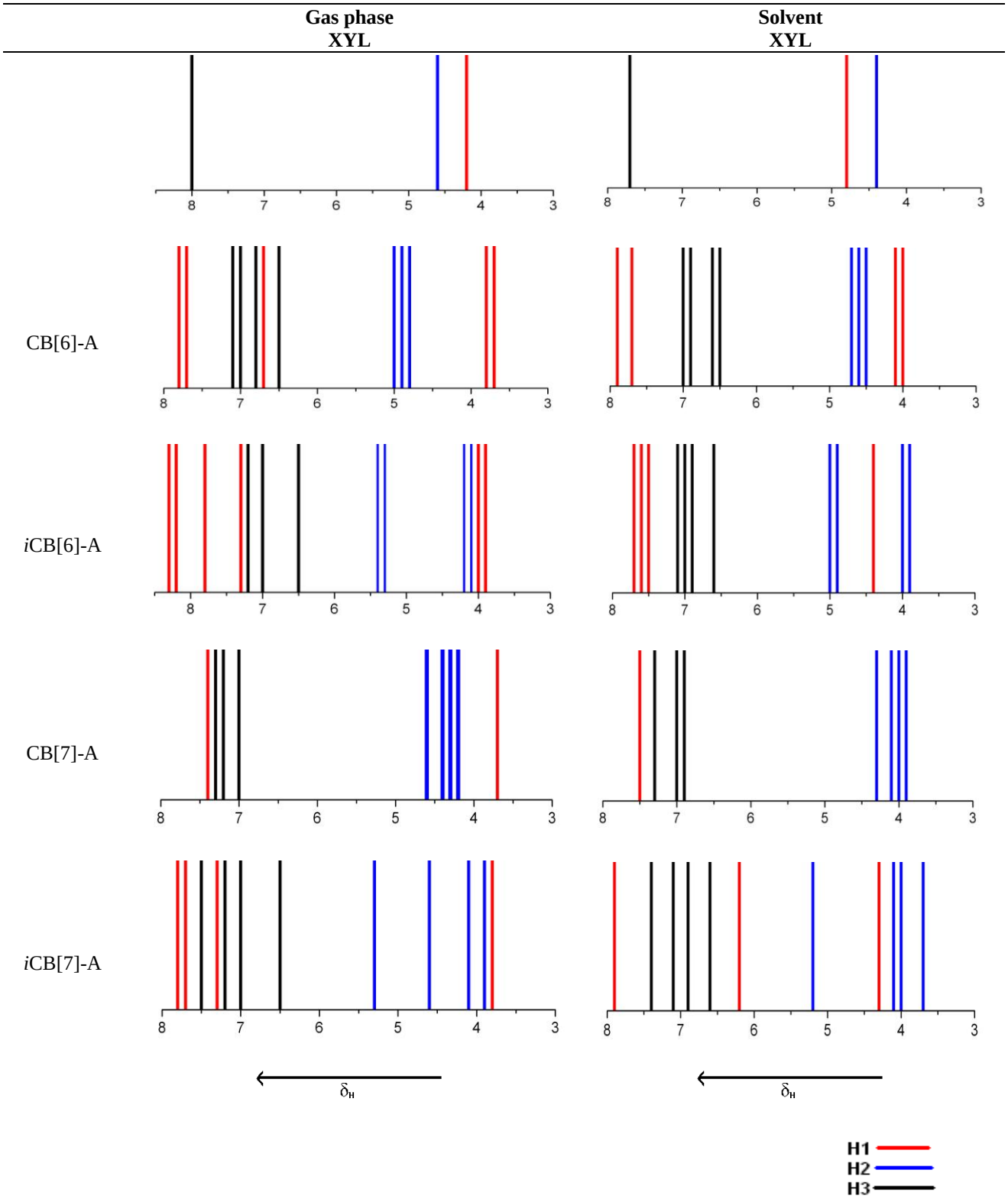
Gas phase
XYL
Solvent
XYL
CB[6]-A
iCB[6]-A
CB[7]-A
iCB[7]-A
8
7
6
5
4
3
δH
H1
H2
H3

Fig. 4(a)

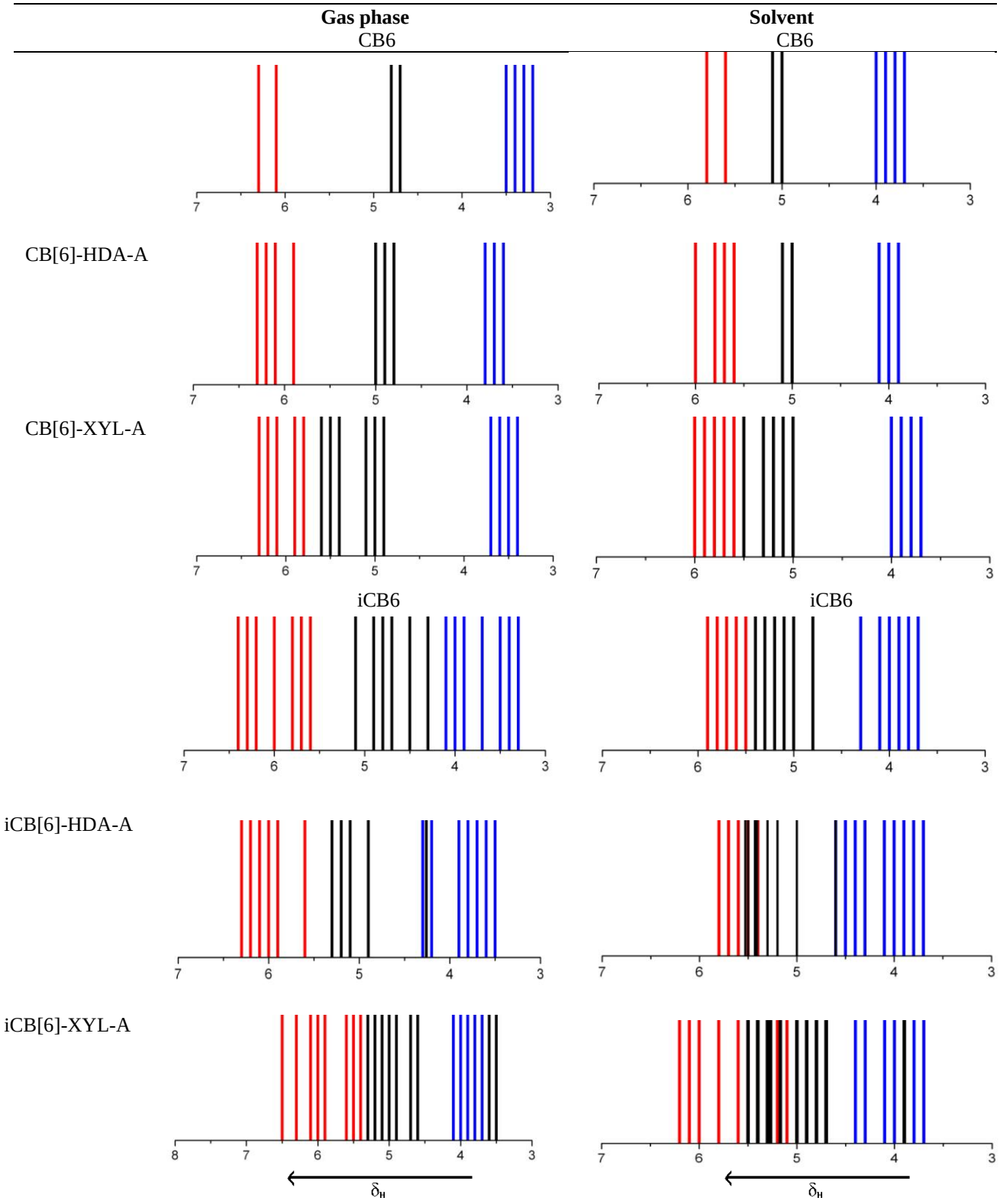
Gas phase
Solvent
CB6
CB6
CB[6]-HDA-A
CB[6]-XYL-A
iCB6
iCB6
iCB[6]-HDA-A
iCB[6]-XYL-A
δH
δH

Fig. 4(b) cont…

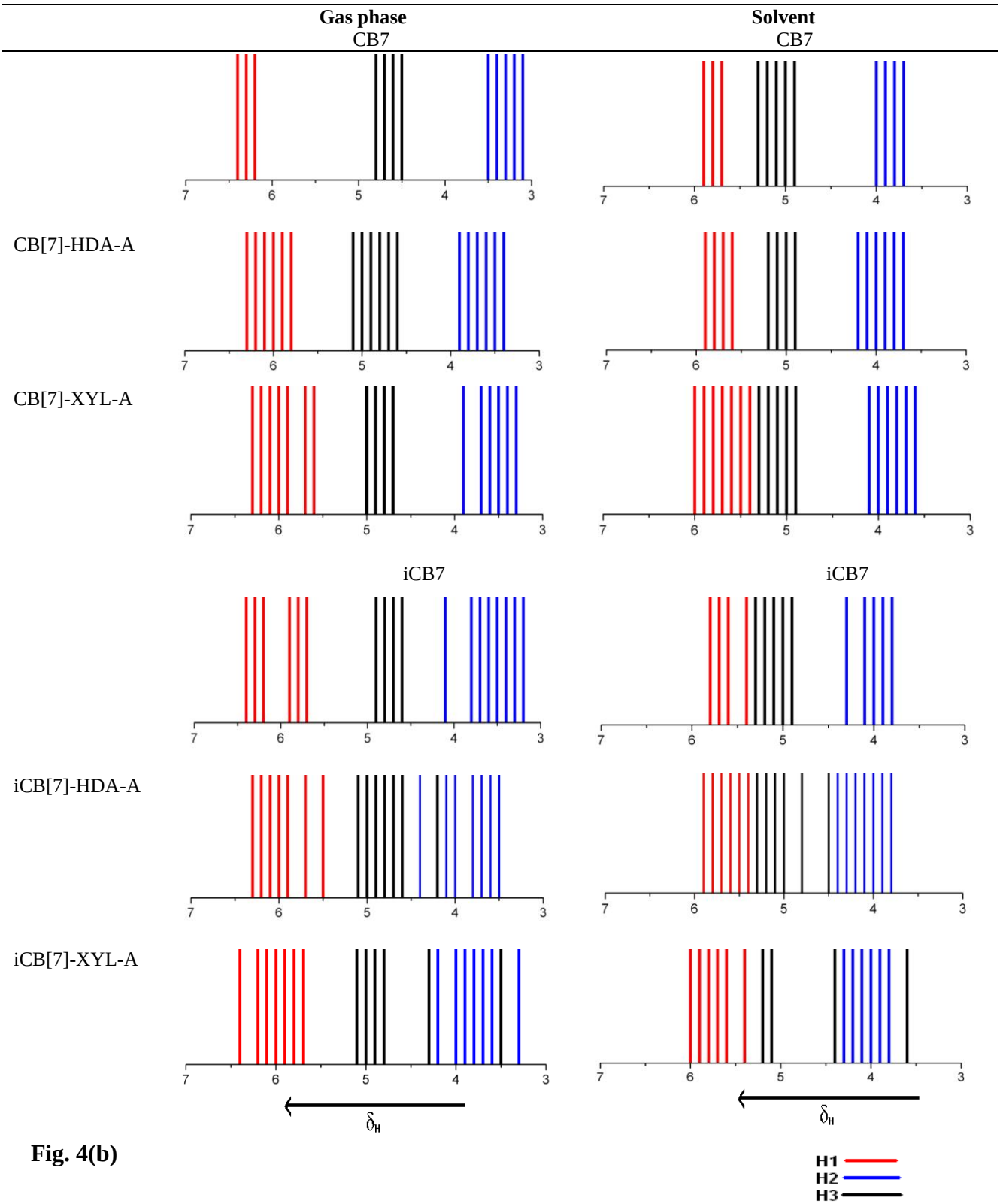
Gas phase
CB7
Solvent
CB7
CB[7]-HDA-A
CB[7]-XYL-A
iCB7
iCB7
iCB[7]-HDA-A
iCB[7]-XYL-A
7
6
5
4
3
δH
H1
H2
H3

Fig. 4(b)